

# SCIENTIFIC REPORTS



OPEN

## Local adaptation to temperature and precipitation in naturally fragmented populations of *Cephalotaxus oliveri*, an endangered conifer endemic to China

Received: 17 December 2015

Accepted: 04 April 2016

Published: 26 April 2016

Ting Wang<sup>1</sup>, Zhen Wang<sup>2</sup>, Fan Xia<sup>3</sup> & Yingjuan Su<sup>3</sup>

*Cephalotaxus oliveri* is an endangered tertiary relict conifer endemic to China. The species survives in a wide range from west to east with heterogeneous climatic conditions. Precipitation and temperature are main restrictive factors for distribution of *C. oliveri*. In order to comprehend the mechanism of adaptive evolution to climate variation, we employed ISSR markers to detect adaptive evolution loci, to identify the association between variation in temperature and precipitation and adaptive loci, and to investigate the genetic structure for 22 *C. oliveri* natural populations. In total, 14 outlier loci were identified, of which five were associated with temperature and precipitation. Among outlier loci, linkage disequilibrium (LD) was high (42.86%), which also provided strong evidence for selection. In addition, *C. oliveri* possessed high genetic variation (93.31%) and population differentiation, which may provide raw material to evolution and accelerate local adaptation, respectively. Ecological niche modeling showed that global warming will cause a shift for populations of *C. oliveri* from south to north with a shrinkage of southern areas. Our results contribute to understand the potential response of conifers to climatic changes, and provide new insights for conifer resource management and conservation strategies.

Global climates including temperatures and precipitation are rapidly changing. The changes of temperature mainly embody in variations in the daily, regional, seasonal, and annual mean temperatures as well as the increase of the intensity, frequency, and duration of abnormally low and high temperatures<sup>1</sup>. The alterations in precipitation primarily reflect in seasonal and temporal variability with the number of precipitation days and the length of dry spells<sup>2</sup>. It is noted that rapid changes in temperature and precipitation exert new selection pressures on plant populations<sup>3</sup>, which strongly influences their physiology, abundance, and distribution<sup>4</sup>. For instance, when plants encounter temperature extremes and extreme events including droughts and storms, flowering which is highly relevant for plant genetic adaptation to climate change is significantly ahead of time<sup>5</sup>. In this context, changes in temperature and precipitation provide an opportunity to investigate plant evolutionary adaptation.

Temperature and precipitation have been revealed as important drivers for local adaptation for conifers<sup>6</sup>. Temperature can profoundly influence seed germination, seedling growth, productivity and distribution of conifers, whereas precipitation has a determinative impact on variables such as soil moisture and the length of a wet or dry season<sup>7,8</sup>. Temporal and spatial variation in temperature and precipitation can also strongly influence the survival of conifers<sup>9</sup>. In extreme situations, high or low temperature stresses and precipitation events will ultimately cause mortality. Thus how to cope with temperature and precipitation becomes particularly important for conifers<sup>10</sup>. Due to their immobility and limited gene flow among populations, conifers locally have to adapt to

<sup>1</sup>College of Life Sciences, South China Agricultural University, Guangzhou 510642, China. <sup>2</sup>College of Sciences, Nanjing Agricultural University, Nanjing 210095, China. <sup>3</sup>School of Life Sciences, Sun Yat-sen University, Guangzhou 510275, China. Correspondence and requests for materials should be addressed to Y.S. (email: suyj@mail.sysu.edu.cn)

fluctuations of temperature and precipitation by change of genotypes<sup>11,12</sup> and inevitably leaves adaptive imprints at the genomic level. Indeed adaptive fingerprints have been widely detected in conifers. For instance, six SNPs in five climate-related candidate genes have been shown under divergent selection between two closely related species *Pinus massoniana* and *Pinus hwangshanensis*<sup>6</sup>. Twenty-three candidate SNPs related to temperature and precipitation have been identified in black spruce (*Picea mariana*)<sup>13</sup>. The prime candidate genes for adaptation to climatic variation involves in a variety of putative functions, including phenology, growth, reproduction, wood formation, lignin metabolism, and stress response<sup>4</sup>. Moreover, conifers also possess specific characteristics such as low domestication, large open-pollinated native populations, and high levels of genetic variation<sup>14</sup>, which makes them particularly valuable for examining local adaptation evoked by temperature and precipitation<sup>14</sup>. Investigating the adaptability of conifers to the two factors may also help to predict their response to future climate change<sup>15</sup>.

*Cephalotaxus oliveri* is an endangered tertiary relict conifer endemic to China with important economical and medical values<sup>16,17</sup>. The plant is ascribed to the Genus *Cephalotaxus* sect. *Pectinate* in Cephalotaxaceae<sup>17</sup>. *Cephalotaxus oliveri* is a wind-pollinated dioecious woody shrubs or small trees up to 4 m tall with yellow to grayish brown and scaly bark. Its distinguishing features embody in leaves densely arranged on leafy shoots and stomatal bands on abaxial surface<sup>17</sup>. Due to deforestation and overexploitation, it has been regarded as a vulnerable species by IUCN<sup>17</sup>. This species is essentially undomesticated and has large geographic ranges including montane regions of northern Guangdong, Guizhou, western Hubei, Hunan, eastern Jiangxi, southern and western Sichuan, and eastern Yunnan in China. Its natural populations have long been disjunctly distributed in subtropical evergreen and deciduous broad-leaved forests, where they occupy humid, shady niches at elevations of 300–1800 m with significant climate heterogeneity<sup>17</sup>. Precipitation and temperature are restrictive factors for the distribution of *C. oliveri*<sup>18</sup>. For instance, precipitation, extremely highest temperature, annual average precipitation, monthly highest average temperature, and annual average temperature have been documented to limit the horizontal and vertical distribution of *Cephalotaxus* in Yunnan<sup>19</sup>. Moreover, temperature can also influence the seed and seedling physiology and morphology<sup>20,21</sup> as well as the speed of seed germination in *Cephalotaxus*<sup>22</sup>. *Cephalotaxus oliveri* was hypothesized to originate in the Oligocene and its population diversification was associated with the rapid uplift of the Qinghai-Tibetan Plateau<sup>23</sup>. The plant has experienced severe changes of temperature and precipitation over the past millions of years and well adapts to cold and arid environment. Hence, *C. oliveri* is suitable for investigating the adaptive evolution mechanism to climate variation. More importantly, in the light of global climate change, it is conducive to understanding the adaptive potential of *C. oliveri* and formulating protection strategy.

Due to the lack of genomic resources for nonmodel species, molecular marker-based genomic scans have been widely used to explore adaptive loci. All loci across the genome are generally expected to share the same demographic history<sup>13</sup>. However, when selective pressures result in strong differentiation of allele frequencies at some loci in the genome<sup>24</sup>, these loci will deviate from the equilibrium model and are considered to be potentially adaptive<sup>25</sup>. Currently, two approaches have been frequently applied to detect adaptive loci. One is Bayescan, which uses Bayesian estimation of the coancestry coefficient  $F_{ST}$  to decide whether a particular locus is adaptive<sup>26,27</sup>. The other is Dfdist, which is mainly a frequentist method based on summary statistics of a symmetrical island model to identify the loci under selection<sup>26,28</sup>. If adaptive loci are further combined with climatic variables, it may be possible to estimate which climatic factors are responsible for adaptive evolution. The association between allele frequency variation and environmental variables can be evaluated by the Spatial Analysis Method (SAM) through logistic regressions<sup>29,30</sup>. The advantages of SAM lie in that it does not depend on genetic models and works at the individual level<sup>29</sup>.

In this study, we employed ISSR markers to detect adaptive loci under selection and utilize SAM to identify the association between climatic variations and genetic data. In addition, we also investigated the genetic structure among natural populations of *C. oliveri*. Because populations sampled represented over a local scale, our results may precisely detect the genetic signatures for adaptation. The goals of the study were (1) to examine adaptive loci in the genome of *C. oliveri*; (2) to analyze the correlation between climatic variables and adaptive loci; (3) to evaluate the population genetic structure of *C. oliveri*, and (4) to explore the genetic basis of the adaptation of *C. oliveri* to climate.

## Results

**Genetic Structure.** Twenty-one ISSR primers were selected to investigate the genetic structure in *C. oliveri* populations. Overall, 310 reliable loci were identified with 100% polymorphic ranging in size from 200 to 2000 bp. A high level of genetic variation was observed with 93.31% polymorphic loci at the species level (Table 1). The highest number of polymorphic loci ( $PPB = 78.8\%$ ,  $H_s = 0.2769$ ,  $I = 0.4125$ ) was exhibited in HNym population and the lowest ( $PPB = 18.44\%$ ,  $H_s = 0.0798$ ,  $I = 0.1141$ ) in JXxs population. At the regional scale, Hunan ( $PPB = 87.88\%$ ,  $H_s = 0.2435$ ,  $I = 0.377$ ) maintained the highest level of variation and Guangdong ( $PPB = 44.67\%$ ,  $H_s = 0.1792$ ,  $I = 0.2607$ ) the lowest. The results indicated that *C. oliveri* possesses a high level of genetic variation.

Populations were significantly structured as revealed by overall  $F_{ST}$  (0.39565) and  $G_{ST}$  (0.3862). AMOVA results further showed that most genetic variation was occurred within populations (60.44%,  $F_{ST} = 0.39565$ ,  $P < 0.001$ ), whereas the proportion of genetic variation among populations within regions was 29.87% ( $F_{SC} = 0.33076$ ,  $P < 0.001$ ) (Table 2). Only 9.7% genetic variation occurred among regions ( $F_{CT} = 0.09696$ ,  $P < 0.001$ ). In addition, significant patterns of isolation by distance were revealed by comparing  $F_{ST}$  values with geographical distances ( $r = 0.571069$ ,  $P < 0.001$ ).

Dendrogram was constructed by the UPGMA method. The results showed that 22 populations of *C. oliveri* were clustered into two groups (Fig. 1). YNdws, the most geographically distant population, was clustered into the separated group. Other 21 populations were clustered into the other group.

Province	Population	Population abbreviation	Geographical coordinate	Altitude (m)	Sample Size	Number of loci	Number of polymorphic loci	Percentage of polymorphic loci	Nei's gene diversity	Shannon's index
Chongqing	Jin Fo Shan	CQjfs	29°01'N 107°05'E	650	15	185	102	0.5514	0.2007	0.2973
	Liang Ping Zhu Shan	CQzs	30°39'N 107°32'E	530	15	193	133	0.6891	0.2156	0.3291
Yunnan	Da Wei Shan	YNdws	27°37'N 113°52'E	2109	15	185	118	0.6378	0.2249	0.334
Sichuan	E Mei Shan	SCems	29°33'N 103°23'E	980	15	173	97	0.5607	0.2089	0.3082
Jiangxi	An Fu	JXaf	27°13'N 114°11'E	420	15	180	131	0.7278	0.2477	0.3712
	Yi Feng	JXyf	28°37'N 114°54'E	741	8	155	62	0.4	0.1477	0.2186
	Xiu Shui	JXxs	28°46'N 114°46'E	307	5	141	26	0.1844	0.0798	0.1141
Hunan	De Hang	HNdh	28°21'N 109°35'E	429	15	190	101	0.5316	0.1782	0.2672
	Hu Ping Shan	HNhps	29°57'N 110°38'E	428–561	15	177	106	0.5989	0.2302	0.3373
	Hui Long	HNhl	28°54'N 110°10'E	399	15	199	136	0.6834	0.2346	0.3514
	Yong Mao	HNym	28°58'N 110°18'E	534	15	184	145	0.788	0.2769	0.4125
	Ha Ni Gong	HNhng	28°56'N 109°57'E	305	15	187	115	0.615	0.2098	0.3145
Guizhou	Wu Yang He	GZwyh	27°03'N 108°18'E	550	15	184	115	0.625	0.2235	0.3324
	Da Sha He	GZdsh	29°04'N 107°24'E	700	15	174	117	0.6724	0.2414	0.359
	Fan Jing Shan	GZjfs	27°49'N 108°36'E	860	15	166	80	0.4819	0.1643	0.246
Guangdong	Dan Xia Shan	GDdxs	25°03'N 113°45'E	800	8	150	67	0.4467	0.1792	0.2607
Hubei	Chang Yang	HBcy	30°43'N 110°54'E	420	15	185	117	0.6324	0.2203	0.3293
	Long Dong	HBld	34°40'N 111°02'E	342	15	176	91	0.517	0.1731	0.2615
	La Mei Xia	HBImx	30°39'N 111°03'E	307	15	179	104	0.581	0.2067	0.3072
	Chai Bu Xi	HBcbx	30°11'N 111°01'E	248	15	187	113	0.6043	0.2076	0.3108
	Hou He	HBhh	30°05'N 110°40'E	440	15	174	86	0.4943	0.1772	0.2629
	Zi Gui Si Xi	HbZg	30°43'N 111°54'E	248	15	182	120	0.6593	0.2141	0.3234
Total					306	269	251	0.9331	0.2214	0.3527

**Table 1.** Origin locations of sampled populations and parameters of genetic diversity revealed by ISSR in *Cephalotaxus oliveri*.

Source of variation	d.f.	Sum of squares	Variance components	Percentage of total variation	P-value	F statistics
Among regions	7	1657.683	2.84409	9.7	<0.001	$F_{CT} = 0.09696$
within regions	14	1972.364	8.76169	29.87	<0.001	$F_{SC} = 0.33076$
Within populations	284	5034.692	17.72779	60.44	<0.001	$F_{ST} = 0.39565$

**Table 2.** AMOVA results for *Cephalotaxus oliveri* populations.

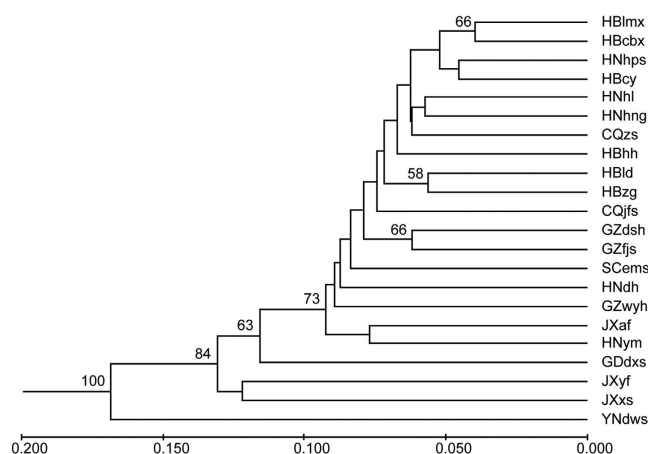


**Figure 1.** UPGMA dendrogram among 22 populations of *C. oliveri* was constructed based on Nei's unbiased genetic distances. Bootstrap values larger than 50% were displayed above branches (% of 1000 replicates). Scale between branch lengths and genetic distances was shown at the bottom of figure.

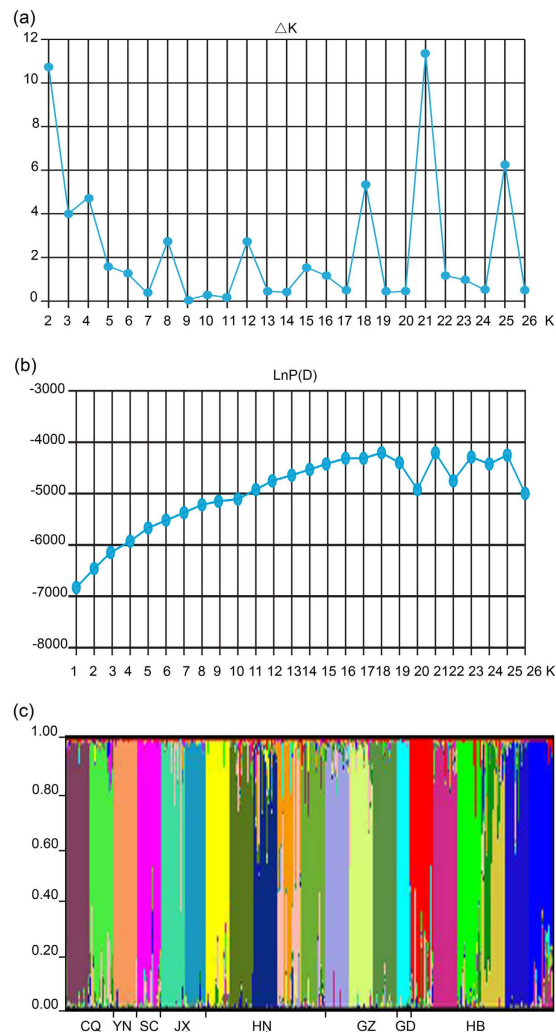


**Figure 2. Bayesian structure analyses of *C. oliveri* populations based on ISSR loci.** (a) Estimates of an ad hoc quantity  $\Delta K$  with respect to  $K$ . The result for  $K=21$  supported by a high  $\Delta K$  value was presented. (b) A plot of the posterior probability of the data ( $\text{LnP}(D)$ ) values for a given  $K$  (1–26). The 21 represented the value of  $K$  with the highest likelihood. (c) Genetic structure of *C. oliveri* in eight regions for  $K=21$  clusters.

$\Delta K$  clearly demonstrated that the uppermost  $K$  equaled 21 (Fig. 2a). The most likely number of genetic clusters  $K$  from STRUCTURE was also 21 (mean  $\text{LnP}(D) = -39912.5$ ,  $\text{Var}[\text{LnP}(D)] = 4877$ ) (Fig. 2b). Populations HBzd and HBld, GZdsh, GZfjs, JXyf, and JXxs were clearly evident, with high proportions of individual assignment to the correct region (Fig. 2c). Only a few populations appeared admixed with others. The results suggested that a high differentiation level existed in *C. oliveri* populations.

**Outlier detection.** Bayescan identified 32 loci as outliers with a  $\log_{10}\text{PO}$  above 2, which is a threshold for decisive evidence for accepting a model under selection, corresponding to a posterior probability greater than 0.99<sup>31</sup> (Fig. 3a). Using the Dfdist, we detected 61 adaptive loci at the 99.5% confidence level (Fig. 3b). Based on two complementary analyses, 14 outlier loci (1, 7, 8, 13, 40, 63, 102, 161, 165, 196, 206, 259, 262, and 300) were identified, which represented truly adaptive loci (Fig. 4a). The very stringent significance criteria in the two approaches also ensured the robustness of 14 outlier loci.

**Linkage disequilibrium.** Linkage disequilibrium (LD) was detected for 28 of the 14225 combinations of all 310 loci with the false discovery rate of 0.1. Twenty of the 310 loci (6.45%) were involved in the detected combinations in LD. In contrast, six (42.86%) of the 14 outlier loci were involved in LD; they were Locus 40, 63, 102, 161, 165, and 206. When two or more linked loci were in LD within a chromosomal region, this region was defined as an LD block<sup>32</sup>. We found that Locus 165 formed LD blocks with nine loci (Locus 130, 135, 144, 149, 150, 151, 152, 154, and 156) (Table 3).

**Association with climatic variables.** The logistic regressions of 310 ISSR markers and 19 climatic variables were calculated using the SAM program. With 99.9999% confidence level, on a total of 6510 models computed,

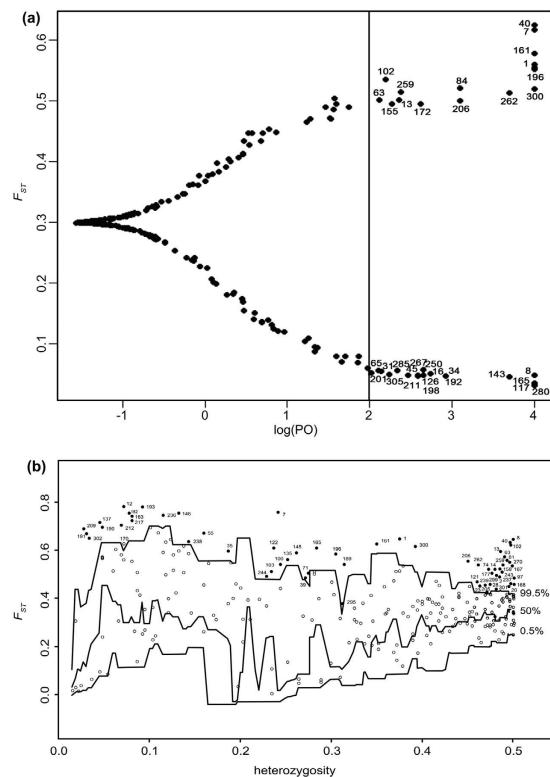


**Figure 3. Outlier loci identified by Bayescan and Dfdist.** (a) Plot of  $F_{ST}$  values and  $\log_{10}PO$  for 310 loci identified using Bayescan. Lines  $\log_{10}PO = 2$  indicate “decisive” evidence for selection corresponding to a posterior probability of 0.99. Solid black dots greater than  $\log_{10}PO 2$  represented outlier loci. (b) Outlier detection performed with Dfdist. Plot of  $F_{ST}$  values of 310 loci in *C. oliveri* populations was against heterozygosity. The 0.5%, 50%, and 99.5% represented confidence intervals, respectively. Loci above the 99.5% line were designated as outlier loci.

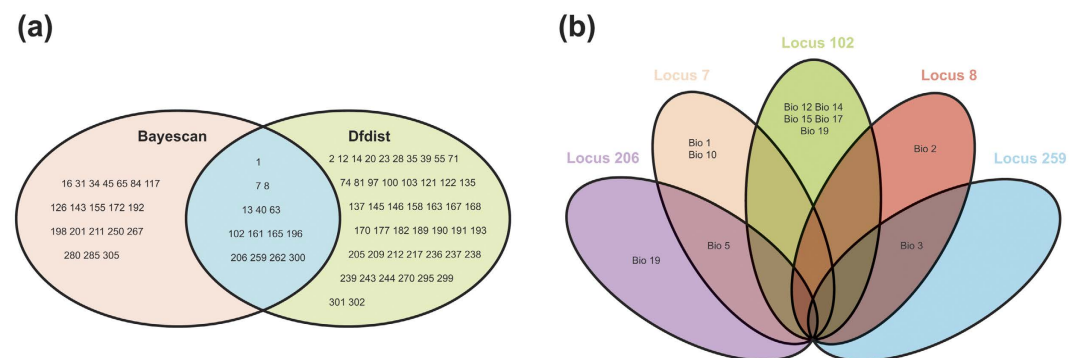


**Figure 4. Number summary of outlier loci and significant association between outliers and climatic variables.** (a) Thirty-two, 61, and 14 outlier loci were detected to be subject selection in *C. oliveri* using Bayescan, Dfdist, and both with Dfdist and Bayescan, respectively. (b) The number association between outliers and climatic variables in SAM analysis. Locus 7 and 8 were significantly associated with three and two temperature variables, respectively. Locus 206 was simultaneously linked to two variables of temperature and precipitation. Locus 102 exhibited 5 significant allele–climate variables. Locus 259 was only linked to one climatic factor.

SAM identified 20 significant associations (0.31%). Of those, ten loci were significantly related with temperature, and 11 were significantly related to precipitation. Furthermore, five of the 20 loci related with climatic factors were also outlier loci detected by Dfdist and Bayescan (Fig. 4b). Locus 7 was significantly associated with annual mean temperature (Bio 1), max temperature of warmest month (Bio 5), and mean temperature of warmest quarter (Bio 10). Locus 8 showed significant association with mean diurnal range (Bio 2) and isothermality (Bio 3). Locus 102 exhibited 5 significant allele–climate variable associations including annual precipitation (Bio 12), precipitation of



Locus	D'	r <sup>2</sup>	p
40 and 34	0.46113208	0.14939114	0.00000002
63 and 53	0.36157921	0.10927404	0.00000002
102 and 79	1.0000	0.10018378	0.00000035
161 and 143	0.78518778	0.12668338	0.00000102
165 and 130	0.82413793	0.2462112	0.00000117
165 and 135	0.50758618	0.24071099	0.00000004
165 and 144	0.91574889	0.13294548	0.00000001
165 and 149	0.46627906	0.02834072	0.00837694
165 and 150	1.00	0.01317884	0.04848577
165 and 151	0.56534094	0.11084024	0.00000369
165 and 152	0.35944977	0.01535935	0.0493768
165 and 154	0.89827126	0.0709272	0.00000371
165 and 156	0.7589286	0.11122229	0.00000039
206 and 180	1.0000	0.16000	0.00000124

**Table 3.** The results of linkage disequilibrium analyzed by TASSAL.

driest month (Bio 14), precipitation seasonality (Bio 15), precipitation of driest quarter (Bio 17), and precipitation of coldest quarter (Bio 19). Locus 206 was significantly associated with max temperature of warmest month (Bio 5) and precipitation of coldest quarter (Bio 19). Locus 259 was linked to isothermality (Bio 3). Loci 7 and 206 were linked to max temperature of warmest month (Bio 5); Loci 8 and 259 were associated with isothermality (Bio 3); Loci 102 and 206 were correlated to precipitation of coldest quarter (Bio 19). Locus 206 was simultaneously linked to temperature and precipitation.

**Potential current and future geographic distribution.** Present and future ecological niche models for *C. oliveri* were estimated by MAXENT (Maximum Entropy Model). The average AUC test for replicate runs and the standard deviation were 0.955 and 0.019, respectively, which indicated good predictive model performance. Minimum training presence logistic threshold was 0.1270. The predicted current geographical distribution of *C. oliveri* was generally similar to its actual distribution including Jiangxi, Hunan, Guizhou, Guangxi, and Hubei, even though some predicted areas do not have any records at present (Fig. 5a). These resulting potential distributions are climatically suitable for *C. oliveri*.

The predicted future and current distribution of *C. oliveri* was considerably different in range. The main difference was that the predicted future suitable area showed a significant reduction in comparison with the current one with a general northward range shift (Fig. 5b,c); the present southern and southeastern regions such as Jiangxi, Hunan, Hubei, and Guangxi were predicted to become significantly unfavorable. Loss of suitable habitats indicated a drastically range contraction (Fig. 5b,c). Populations of *C. oliveri* may become more patchily distributed than at present.

## Discussion

This study has analyzed the adaptive evolution of *C. oliveri* to temperature and precipitation through ISSR markers (Inter-Simple Sequence Repeats). ISSRs are highly variable and have been widely applied to the assessment of population genetic diversity and structure in plants<sup>33,34</sup>. However, ISSRs were seldom used to detect adaptive loci in genome. Currently, the most efficient approach to identify candidate genomic regions under selection is AFLP (Amplified Fragment Length Polymorphism) based on PCR (Polymerase Chain Reaction) to obtain amplified polymorphisms<sup>35</sup>. Similar to AFLP, ISSR can also generate a large number of polymorphic loci in genome without prior sequence information<sup>33,36,37</sup>. Although ISSR are assumed to be neutral markers, its primers also can match to microsatellite regions and genes encoding specific proteins<sup>33,38,39</sup>. Hence ISSR is suitable for detecting candidate loci under selection.

We first applied ISSRs to identify adaptive evolution in *C. oliveri* and ascertain the relationships between candidate loci and climatic factors. In order to ensure unbiased analysis, only distinct, reproducible ISSR loci were scored in this study. Three hundred and ten loci produced by 21 primers have good genome coverage in *C. oliveri*. Fourteen outlier loci were identified by both Dfdist and Bayescan. The two complementary and exhaustive methods guaranteed strong confidence of the 14 loci with very stringent significance criteria. The proportion of outlier loci detected in *C. oliveri* was 4.22%, which conformed to the percentage between 2% to 15% in AFLP genome scan or other molecular markers<sup>40</sup>. For instance, 2.9% in *Mikania micrantha* from AFLP<sup>35</sup>, 3% in Norway spruce (*P. abies*) from RAPD markers<sup>41</sup>, and 3.7% in white spruce from SNPs<sup>42</sup>.

Temperature and precipitation have been identified to be the major selective pressure driving plant adaptation<sup>8,9,43,44,45</sup>. The two climatic factors are very important for plant growth, development, survival, reproduction and defense<sup>8</sup>. Currently, adaptive loci associated with temperature and precipitation have been detected in plants<sup>9</sup>. For instance, the close relationship between AFLP allele frequencies and temperature and precipitation have been found in *P. monticola* and *Keteleeria davidiana* var. *formosana*<sup>9,43,46</sup>. Nine SNPs associated with climate-related complex trait variation have also been identified in Sitka spruce (*P. sitchensis*)<sup>47</sup>. SNPs associated with seasonal minimum temperatures are detected in four conifers, *Abies alba*, *Larix decidua*, *P. cembra*, and *P. mugo*, whereas SNPs in *L. decidua* and *P. cembra* are found to be related to seasonal maximum temperature and winter and

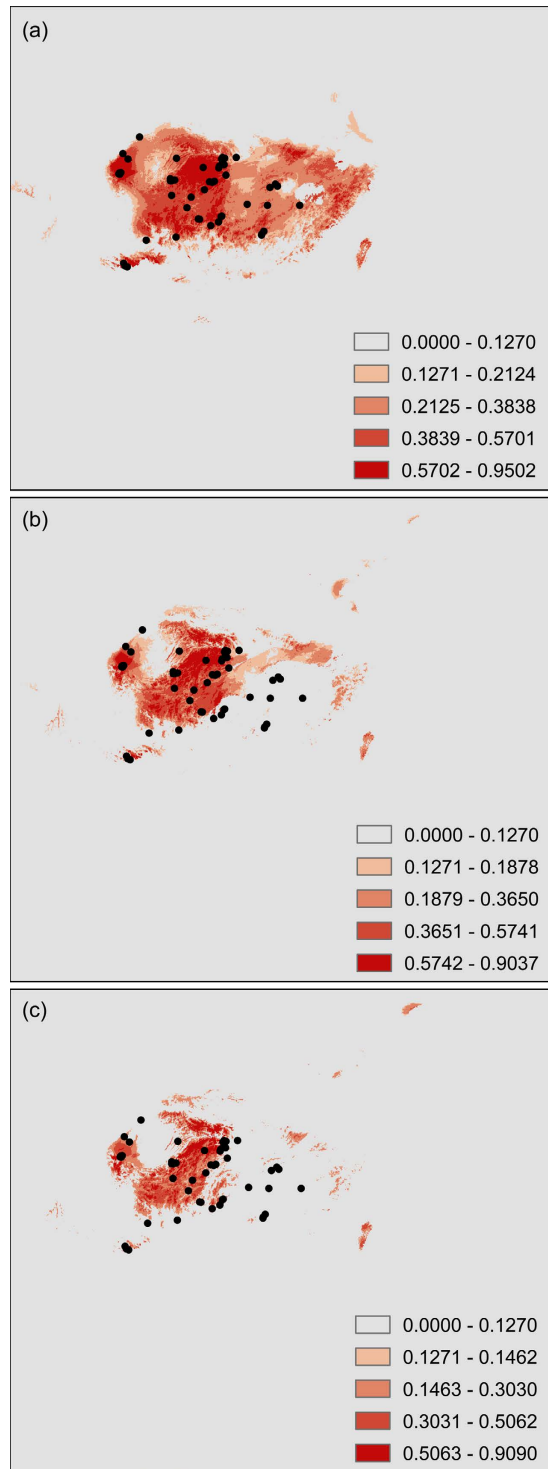


**Figure 5. Potential current and future distributions inferred from ecological niche modeling (Program MAXENT 3.3.3k, URL <http://www.cs.princeton.edu/~schapire/maxent/>) for *C. oliveri* in China based on WorldClim variables. Two climate scenarios IPCC-CMIP5 RCP 4.5 and RCP 8.5 under HadGEM2-ES model were used to ensure the accuracy of evaluation on future distribution. (a) Predicted current distribution of *C. oliveri* based on climate grids for the periods 1950–2000. (b) Possible future distribution of *C. oliveri* in 2070 based on RCP 4.5 climate scenario. (c) Projected future distribution of *C. oliveri* in 2070 based on RCP 8.5 climate scenario.**

autumn precipitations<sup>48</sup>. The local polymorphism patterns of candidate genes linked to drought tolerance has also been detected in a widespread Mediterranean conifer (*P. halepensis*)<sup>49</sup>. As restrictive factors, temperature and precipitation were suggested to strongly influence the geographical distribution of *C. oliveri*<sup>18</sup>. In this study, five

among 14 outlier loci were also revealed to be associated with temperature or precipitation. Local climatic conditions impacted 1.6% of ISSR loci in *C. oliveri*, suggesting that a relatively small number of loci govern climatic adaptation in this species. The result was very similar to previous studies<sup>13,50</sup>. Twenty-two adaptive loci associated with climatic variables was identified in Loblolly pine (*P. taeda*)<sup>50</sup>, whereas ten outlier loci were detected in black spruce (*P. mariana*)<sup>13</sup>. Their proportions of detected loci associated with the climatic variables were 1.3% and 1.7%, respectively.

Furthermore, we found that one adaptive locus simultaneously was linked to temperature and precipitation. The result indicated that the candidate locus might have undergone the same selective pressures<sup>51</sup>. The same phenomenon was also demonstrated in black spruce (*P. mariana*), whose four of 26 outlier SNPs were common to both the temperature and the precipitation<sup>13</sup>. It has been noted that physiological processes involved in adaptation to temperature and precipitation may be related in conifers<sup>52,53</sup>. In *P. abies*, drought tolerance was found to be genetically correlated with tolerance to freezing temperature<sup>53</sup>. In *P. mariana*, a gene coding for the DnaJ heat shock protein was detected to carry an adaptive SNP related to both temperature and precipitation, and the protein was produced under stresses involving temperature and moisture<sup>10</sup>. In whitebark pine (*P. albicaulis*) and loblolly pine (*P. taeda*), annual, seasonal mean temperatures, and rainfall patterns also appear to drive local adaptation, which primarily involved response to both temperature and drought<sup>50,54</sup>. *Cephalotaxus oliveri* extends from the west to the east in China, with an environmental gradient showing significant precipitation and temperature differences<sup>55</sup>. The finding of adaptive loci implies that *C. oliveri* has successfully responded and adapted to historic climate changes. The species was inferred to originate in the Oligocene [ca. 28.32 million years ago (Ma)] and diversified in the early Miocene (ca. 17.73 Ma)<sup>23</sup>. In the long evolutionary process, the high genetic variation possessed by *C. oliveri* may have provided raw material for its adaptation to changing climatic conditions. Meanwhile, its high population differentiation possibly also accelerated local adaptation. Our results indicated that *C. oliveri* populations well adapt to temperature and precipitation factors including annual mean temperature (Bio 1), mean diurnal range (Bio 2), isothermality (Bio 3), max temperature of warmest month (Bio 5), mean temperature of warmest quarter (Bio 10), annual precipitation (Bio 12), precipitation of driest month (Bio 14), precipitation seasonality (Bio 15), precipitation of driest quarter (Bio 17), and precipitation of coldest quarter (Bio 19) (Fig. 4b).

The geographic pattern also provided a useful indication of adaptive variation<sup>56,57</sup>. The natural populations of *C. oliveri* have a wide geographic range, from south to north is from 25°3′N, 130°45′E to 34°40′N, 111°02′E and east to west from 28°37′N, 114°54′E to 27°37′N, 113°52′E (Table 1). Within the range, *Cephalotaxus oliveri* has to face with a great climate variation, including subtropical monsoon climate, East Asian humid monsoon climate, subtropical mountain monsoon humid climate, and eastern humid mountain monsoon climate, respectively<sup>55</sup>, which results in seasonal difference of precipitation. Water availability is one of the major abiotic stressors that can lead to adaptive variation in conifers<sup>50</sup>. Specifically, lack of precipitation during winter period represents a great threat to conifers<sup>58</sup>. In line with this, precipitation of coldest quarter becomes the most often climate variable that was detected in the significant allele-environment associations<sup>57</sup>. In this study, SAM analysis further showed that precipitation of coldest quarter was one of the factors driving the adaptive evolution of *C. oliveri*, which was consistent to the previous ecological hypothesis<sup>55</sup>.

Linkage disequilibrium (LD) in the genomic region can reflect the genetic signature associated with local adaptation, especially for long-lived plants<sup>51,59</sup>. Here we observed that of all the 310 loci examined for *C. oliveri*, only twenty (6.45%) were found to be involved in LD. Our result lends further support to the theory that LD in forest trees decays rapidly<sup>60</sup>. However, if only considering outlier loci, the proportion (42.86%) of loci involved in LD was relatively high. This is not unexpected as strong positive selection may increase the frequency of an advantageous allele, causing linked loci remain in strong LD with that allele (genetic hitch-hiking)<sup>59</sup>. More importantly, Locus 165 was identified to form LD blocks with nine loci. The significant LD among the loci reflect that they may not only have experienced the same selection pressure, but also have been acted upon by evolutionary mechanisms like co-adaptation of gene complexes<sup>51,61</sup>. The LD blocks implies potential genomic regions that are associated with adaptations.

It is also worthy of note that for the pairwise LD analysis between Locus 102 and 79, 165 and 150, and 206 and 180, the two statistics  $D'$  and  $r^2$  acted quite differently; namely,  $D'$  had a value of 1, but  $r^2$  were much smaller (Table 3). This performance difference is due to the fact that  $D'$  and  $r^2$  reflect different aspects of LD<sup>62</sup>.  $D'$  measured only recombinational history, whereas  $r^2$  summarized both recombinational and mutational history. The results of *C. oliveri* indicated that the polymorphisms between the three pairs of locus were not completely correlated, but there was no evidence of recombination.

We used MAXENT to project the distribution of *C. oliveri* under current and future climate conditions. MAXENT captured well a major portion of current distribution of *C. oliveri* in China and also deduced its future range under a climatic warming scenario. With a rate of rising of 0.1 °C–0.4 °C per decade<sup>63</sup>, future temperature was assumed to increase by 2.3 °C–2.7 °C in 2070. As a result, the projection predicted that *C. oliveri* will lose considerable suitable areas with climate warming. Similar predictions have been made for other tree species<sup>54,64,65</sup>. More specifically, the southern and southeastern populations of *C. oliveri* were projected to be more sensitive to climate warming than others. This information is quite helpful for formulating a protection strategy when considering future climate conditions. Although *C. oliveri* possesses high levels of population genetic variation, its long generation time and limited seed dispersal will constrain adaptations to rapid climate change<sup>54,64,66,67</sup>. On the other hand, at the regional scale Hunan had the highest ISSR variation, whereas the lowest was found in Guangdong. In our previous research, the similar variation pattern has also been revealed for *C. oliveri* populations based on *trnL-F*, *atpB-rbcL* and *trnD-trnT* sequences<sup>23</sup>. Population HN<sub>hps</sub> was recognized as the refugium during the Pleistocene ice ages, and populations in Guangdong were speculated to expand from Hunan<sup>23</sup>. In conjunction with the MAXENT predictions, the population genetic data will be used to develop an ex situ conservation action plan for *C. oliveri*.



In summary, this is the first study examining the adaptive loci, relationship between outliers and climatic factors, and the underlying mechanisms of local adaptation in *C. oliveri*. Our results indicated that *C. oliveri* exhibits remarkable adaptations to temperature and precipitation. Global warming may profoundly affect its viability and distribution. In the next steps we will dissect the adaptive value of the identified loci by sequencing and gene analysis in order to further understand the adaptation of *C. oliveri* to climatic factors.

## Methods

**Sample collection.** Twenty-two naturally fragmented populations of *Cephalotaxus oliveri* were collected from the whole distribution range of the species (Table 1). Population samples contained five to fifteen individuals (Table 1). All selected populations except JXxs, JXyf, and GDdxs had 15 individuals, which were randomly sampled with 10–20 m interval. If the population size was less than 15, all individuals were collected. Young, healthy leaves were collected and dried in silica gel in zip-lock plastic bags until DNA extraction. Vouchers were deposited at the Herbarium of Sun Yat-sen University (SYSU), Guangzhou, China.

**Climatic data collection.** Climatic layers at 2.5' resolution for current conditions were obtained from the WorldClim database (<http://www.worldclim.org/>)<sup>68</sup>. The 19 bioclimatic variables were extracted by DIVA-GISv7.5 software (<http://www.diva-gis.org/>) in terms of informatic characterization of *C. oliveri*. The bioclimatic variables included annual mean temperature (Bio 1), mean diurnal range (Bio 2), Isothermality (Bio 3), temperature seasonality (Bio 4), max temperature of warmest month (Bio 5), min temperature of coldest month (Bio 6), temperature annual range (Bio 7), mean temperature of wettest quarter (Bio 8), mean temperature of driest quarter (Bio 9), mean temperature of warmest month (Bio 10), mean temperature of coldest month (Bio 11), annual precipitation (Bio 12), precipitation of wettest month (Bio 13), precipitation of driest month (Bio 14), precipitation seasonality (Bio 15), precipitation of wettest quarter (Bio 16), precipitation of driest quarter (Bio 17), precipitation of warmest quarter (Bio 18), and precipitation of coldest quarter (Bio 19) (Supplementary Table S1).

**DNA extraction.** We extracted genomic DNA from tissues using a modified cetyltrimethyl ammonium bromide (CTAB) method with  $-20^{\circ}\text{C}$  propanone pretreatment to eliminate polysaccharides, which was successful for conifers<sup>34,69</sup>. The DNA was stored at  $-20^{\circ}\text{C}$  until further use.

**ISSR amplification.** To cover the widest genomic region and ensure high-quality reproducible bands, an initial screening was developed using one individuals randomly obtained from HNhng population. Twenty-one primers were screened from 100 primers (UBC primer set #9) of the Biotechnology Laboratory, University of British Columbia. PCR amplification was carried out in a total volume of 20  $\mu\text{l}$  consisting of 20 ng of template DNA, 10 mM Tris-HCl (pH 8.3) reaction buffer, 50 mM KCl, 2.0 mM  $\text{MgCl}_2$ , 0.25 mM dNTPs, 0.24  $\mu\text{M}$  primer, 1.5 units of *Taq* polymerase, and DNA-free water. In an ABI veriti thermocycler, PCR started with an initial denaturation at  $94^{\circ}\text{C}$  for 5 min followed by 40 cycles with  $94^{\circ}\text{C}$  for 30 s,  $53^{\circ}\text{C}$ – $54^{\circ}\text{C}$  for 45 s and  $72^{\circ}\text{C}$  for 90 s, and ended with a final extension of 7 min at  $72^{\circ}\text{C}$ . DNA quality and quantity were estimated using 1.7% agarose gel in TAE 1X buffer, stained with Ethidium Bromide. Additionally, 100 bp ladder and negative and positive controls were loaded and run at constant voltage (135 V) for 95 min. After running, the gels were UV visualized and recorded using a Gel Doc 2000 Camera.

**Data Analysis.** Unambiguous ISSR fragments were transformed into 01 character matrix (1 = presence, 0 = absence).

POPGENE ver 1.31 was used to calculate genetic parameters. The estimates included the percentage of polymorphic loci (P), Nei's (1973) gene diversity (H), Shannon's information index (I), total gene diversity (Ht), and gene differentiation ( $G_{ST}$ )<sup>70</sup>.

The variation among and within 22 populations were performed by analysis of molecular variance (AMOVA) with 1000 permutations using ARLEQUIN version 3.0<sup>71,72</sup>. Using the same software, a Mantel test<sup>72</sup> was conducted to analyze the relationship between pairwise population genetic and geographic distances. Genetic distances were computed as pairwise  $F_{ST}$  values between all pairs of populations<sup>73</sup>. The unweighted pair group method (UPGMA) based on Nei's unbiased (1978) genetic distance<sup>74</sup> was performed using the TFPGA 1.3 program for constructing a dendrogram to reveal the genetic relationship among populations<sup>75</sup>. Bootstrap values for nodes were estimated based on 1000 replications.

To infer population structure, we assigned individuals and populations to clusters by using the model-based program STRUCTURE 2.3<sup>76</sup>. Thirty independent runs for each value of  $K = 1$ –27 were conducted to estimate the number of clusters ( $K$ ) with maximum likelihood with the following settings: admixture model, correlated allele frequencies, burn-in length of 100 000, MCMC repetitions of 1000<sup>77</sup>, and ten times of iterations. A best-estimated  $K$  was defined both using log probabilities [ $\text{Pr}(X|K)$ ] and hoc statistic  $\Delta K$ <sup>78</sup>.

To identify loci under selection, software Dfdist and Bayescan were used to ensure truly adaptive regions of the genome. The software Dfdist was applied to simulate a null distribution of  $F_{ST}$  values under an island model, which was insensitive to population structure, demographic structure and mutation level. Simulations were computed with a mean  $F_{ST}$  similar to the trimmed mean  $F_{ST}$ , which was calculated by excluding 30% of the most extreme  $F_{ST}$  values observed in the empirical dataset. We compared the distributions of the  $F_{ST}$  values over all loci to null hypothesis of neutral evolution. Loci with a high or low  $F_{ST}$  value were considered as potentially under selection. In this study, we simulated the neutral distribution of  $F_{ST}$  with 50 000 iterations at the 99.5% confidence level. Bayescan developed by Foll and Gaggiotti<sup>27</sup> is an  $F_{ST}$  based model, which uses reversible jump MCMC and estimation of the Bayesian posterior probability<sup>26</sup>. It searches for loci with extreme  $F_{ST}$  values. Large  $F_{ST}$  is then interpreted as signature of local adaptation. We calculated outliers using a burn-in of 50 000 iterations, a thinning interval of 20, and a sample size of 5 000.

Linkage disequilibrium (LD) between all pairs of ISSR loci was calculated by the squared allele frequency correlation coefficient ( $r^2$ ) implemented in TASSEL 2.2 (Trait Analysis by aSSociation, Evolution, and Linkage)<sup>79</sup>. The pair-wise significance was computed by 1,000 permutations after removal of loci with rare alleles ( $f < 0.05$ ).

The evaluated estimates included the standardized disequilibrium coefficient ( $D'$ ), as well as the squared correlation coefficient ( $r^2$ ) and  $p$  values based on Fisher's exact test.  $D'$  determined whether recombination had occurred between a pair of alleles<sup>80</sup>. The critical value of  $r^2$  was the conventional 0.1<sup>81</sup>. Statistical tests for each  $r^2$  were provided by the  $p$  value calculated in TASSEL.

To investigate the association between ISSR genetic data and climatic variables, SAM was employed (available at <http://www.econogene.eu/software/sam>). The likelihood ratio ( $G$ ) and Wald tests were used to determine the significance of the models. The null hypothesis was designed so that the above two statistical parameters conformed to a normal distribution. A model was considered significant only if the null hypothesis was rejected by both statistical tests at the 95 and 99.999% confidence level. The 310 ISSR markers in all 22 *C. oliveri* populations were examined against 19 climatic variables in the SAM analysis.

We used MAXENT 3.3.3k<sup>82</sup> to predict distribution changes for *C. oliveri* as a result of climate warming. MAXENT is a program for maximum entropy modelling of the geographical distributions of species; it combines presence-only data with ecological-climatic layers to predict suitable areas. For current distribution, we down-scaled climate grids for the periods 1950–2000. In addition to sample locations in this study, we also collected the distribution records of *C. oliveri* from the Chinese Virtual Herbarium (<http://www.cvh.org.cn/>). After removing duplicate records, it remained a total of 57 records of *C. oliveri* that were used to generate the distribution model by using 19 bioclimatic data layers from the WorldClim database (<http://www.worldclim.org>) at 2.5-arcmin resolution (Supplementary Table S1).

We selected the Hadley Global Environment Model 2 (HadGEM2-ES) as a general circulation model under two climate scenarios (IPCC-CMIP5 RCP 4.5/8.5) to ensure the accuracy of evaluation. The RCP 8.5 scenario represents a higher predicted greenhouse gas emission than RCP 4.5<sup>83</sup> (Supplementary Tables S2–S3).

MAXENT was run according to the following settings: random test percentage = 25; regularization multiplier = 1; convergence threshold = 0.00001; maximum iterations = 1000 and averaged across 10 cross-validation runs. Ultimately, variable importance was determined by a jackknife test. We evaluated the accuracy of each model prediction by calculating the area under the curve (AUC) values. AUC is an efficient indicator of model performance<sup>84</sup>. AUC values > 0.9 indicates high reliability of the model<sup>85</sup>.

## References

1. Yamori, W., Hikosaka, K. & Way, D. A. Temperature response of photosynthesis in C-3, C-4, and CAM plants: temperature acclimation and temperature adaptation. *Photosynth. Res.* **119**, 101–117 (2014).
2. Jongen, M. *et al.* Resilience of montado understorey to experimental precipitation variability fails under severe natural drought. *Agr. Ecosyst. Environ.* **178**, 18–30 (2013).
3. Hoffmann, A. A. & Sgrò, C. M. Climate change and evolutionary adaptation. *Nature* **470**, 479–85 (2011).
4. Franks, J. S. & Hoffmann, A. A. Genetics of climate change adaptation. *Annu. Rev. Genet.* **46**, 185–208 (2012).
5. Parmesan, C. & Yohe, G. A globally coherent fingerprint of climate change impacts across natural systems. *Nature* **421**, 37–42 (2003).
6. Zhou, Y. F., Zhang, L. R., Liu, J. Q., Wu, G. L. & Savolainen, O. Climatic adaptation and ecological divergence between two closely related pine species in Southeast China. *Mol. Ecol.* **23**, 3504–3522 (2014).
7. Concilio, A., Chen, J. Q., Ma, S. & North, M. Precipitation drives interannual variation in summer soil respiration in a Mediterranean-climate, mixed-conifer forest. *Climatic Change* **92**, 109–122 (2009).
8. Poncet, B. N. *et al.* Tracking genes of ecological relevance using a genome scan in two independent regional population samples of *Arabis alpina*. *Mol. Ecol.* **19**, 2896–2907 (2010).
9. Manel, S. *et al.* Broad-scale adaptive genetic variation in alpine plants is driven by temperature and precipitation. *Mol. Ecol.* **21**, 3729–3738 (2012).
10. Prunier, J., Gérardi, S., Laroche, J., Beaulieu, J. & Bousquet, J. Parallel and lineage-specific molecular adaptation to climate in boreal black spruce. *Mol. Ecol.* **21**, 4270–4286 (2012).
11. Kiani, S. P. *et al.* Allelic heterogeneity and trade-off shape natural variation for response to soil micronutrient. *PLoS Genet.* **8**, e1002814 (2012).
12. Alberto, F. J. *et al.* Potential for evolutionary responses to climate change evidence from tree populations. *Global Change Biol.* **19**, 1645–1661 (2013).
13. Prunier, J., Laroche, J., Beaulieu, J. & Bousquet, J. Scanning the genome for gene SNPs related to climate adaptation and estimating selection at the molecular level in boreal black spruce. *Mol. Ecol.* **20**, 1702–1716 (2011).
14. González-Martínez, S. C., Krutovsky, K. V. & Neale, D. B. Forest-tree population genomics and adaptive evolution. *New Phytol.* **170**, 227–238 (2006).
15. de Luis, M. *et al.* Plasticity in dendroclimatic response across the distribution range of Aleppo Pine (*Pinus halepensis*). *PLoS One* **8**, e83550 (2013).
16. Fu, L. G. & Jin, J. M. *Red list of endangered plants in China*. (Science Press, 1992).
17. Fu, L. G., Li, N. & Mill, R. R. *Cephalotaxaceae*. In *Flora of China* (eds Wu, Z. Y. & Raven, P. H.) 85–88 (Science Press, Beijing and Missouri Botanical Garden Press, 1999).
18. Ai, Q. F., Chen, M. H. & Liang, X. Research progress on *Cephalotaxus oliveri*. *Guizhou Agric. Sci.* **3**, 55 (2010).
19. Sima, Y. K., Yu, H., Yang, G. Y. & Zhao, W. S. The relation between Yunnan geographic distribution of *Cephalotaxus* and environment. *For. Invent. Plann.* **29**, 83–87 (2004).
20. Jiao, Y. L., Zhou, Z. C., Jin, G. Q. & Li, Y. G. *Cephalotaxus fortunei* seed-physiological changes and differences among three seed sources during low temperature priming. *J. Zhejiang For. Coll.* **24**, 173–178 (2007).
21. Jiao, Y. L. *et al.* Provenance differences for seedling morphology and growth of *Cephalotaxus fortunei*. *For. Res.* **19**, 452–456 (2006).
22. Yang, C. J. *et al.* Deep simple morphophysiological dormancy in seeds of the basal taxad *Cephalotaxus*. *Seed Sci. Res.* **21**, 215–226 (2011).
23. Wang, C. B., Wang, T. & Su, Y. J. Phylogeography of *Cephalotaxus oliveri* (Cephalotaxaceae) in relation to habitat heterogeneity, physical barriers and the uplift of the Yungui Plateau. *Mol. Phylogeny. Evol.* **80**, 205–216 (2014).
24. Coop, G., Witonsky, D., Di Rienzo, A. & Pritchard, J. K. Using environmental correlations to identify loci underlying local adaptation. *Genetics* **185**, 1411–1423 (2010).

25. Pyhäjärvi, T., Hufford, M. B., Mezouk, S. & Ross-Ibarra, J. Complex patterns of local adaptation in teosinte. *Genome Biol. Evol.* **5**, 1594–1609 (2013).
26. Beaumont, M. A. & Balding, D. J. Identifying adaptive genetic divergence among populations from genome scans. *Mol. Ecol.* **13**, 969–980 (2004).
27. Foll, M. & Gaggiotti, O. A genome-scan method to identify selected loci appropriate for both dominant and codominant markers: A Bayesian perspective. *Genetics* **180**, 977–993 (2008).
28. Beaumont, M. A. & Nichols, R. A. Evaluating loci for use in the genetic analysis of population structure. *Proc. R. Soc. Lond. B-Biol. Sci.* **263**, 1619–1626 (1996).
29. Joost, S. *et al.* A spatial analysis method (SAM) to detect candidate loci for selection: towards a landscape genomics approach to adaptation. *Mol. Ecol.* **16**, 3955–3969 (2007).
30. Joost, S., Kalbermatten, M. & Bonin, A. Spatial analysis method(SAM): a software tool combining molecular and environmental data to identify candidate loci for selection. *Mol. Ecol. Resour.* **8**, 957–960 (2008).
31. Fischer, M. C., Foll, M., Excoffier, L. & Heckel, G. Enhanced AFLP genome scans detect local adaptation in high-altitude populations of a small rodent (*Microtus arvalis*). *Mol. Ecol.* **20**, 1450–1462 (2011).
32. Xie, C. X. *et al.* An analysis of population structure and linkage disequilibrium using multilocus data in 187 maize inbred lines. *Mol. Breed.* **21**, 407–418 (2008).
33. Thorogood, C. J., Rumsey, F. J., Harris, S. A. & Hiscock, S. J. Host-driven divergence in the parasitic plant *Orobanchaceae*. *Mol. Ecol.* **17**, 4289–4303 (2008).
34. Su, Y. J., Wang, T. & Ouyang, P. Y. High genetic differentiation and variation as revealed by ISSR marker in *Pseudotsaxus chienii* (Taxaceae), an old rare conifer endemic to China. *Biochem. Syst. Ecol.* **37**, 579–588 (2009).
35. Wang, T., Chen, G. P., Zan, Q. J., Wang, C. B. & Su, Y. J. AFLP genome scan to detect genetic structure and candidate loci under selection for local adaptation of the invasive weed *Mikania micrantha*. *PLoS One* **7**, e41310 (2012).
36. Henry, R. J. *Plant genotyping: the DNA fingerprinting of plants*. (CABI Publishing, 2001).
37. Mort, M. E. *et al.* Relationships among the Macaronesian members of *Tolpis* (Asteraceae: Lactuceae) based upon analyses of inter simple sequence repeat (ISSR) markers. *Taxon* **52**, 511–518 (2003).
38. Storz, J. F., Payseur, B. A. & Nachman, M. W. Genome scans of DNA variability in humans reveal evidence for selective sweeps outside of Africa. *Mol. Biol. Evol.* **21**, 1800–1811 (2004).
39. Minder, A. M. & Widmer, A. A population genomic analysis of species boundaries: neutral processes, adaptive divergence and introgression between two hybridizing plant species. *Mol. Ecol.* **17**, 1552–1563 (2008).
40. Meyer, C. L., Vitalis, R., Saumitou-Laprade, P. & Castric, V. Genomic pattern of adaptive divergence in *Arabidopsis halleri*, a model species for tolerance to heavy metal. *Mol. Ecol.* **18**, 2050–2062 (2009).
41. Acheré, V., Favre, J. M., Besnard, G. & Jeandroz, S. Genomic organization of molecular differentiation in Norway spruce (*Picea abies*). *Mol. Ecol.* **14**, 3191–3201 (2005).
42. Namroud, M. C., Beaulieu, J., Juge, N., Laroche, J. & Bousquet, J. Scanning the genome for gene single nucleotide polymorphisms involved in adaptive population differentiation in white spruce. *Mol. Ecol.* **17**, 3599–3613 (2008).
43. Richardson, B. A., Rehfeldt, G. E. & Kim, M. S. Congruent climate-related genecological responses from molecular markers and quantitative traits for western white pine (*Pinus Monticola*). *Int. J. Plant Sci.* **170**, 1120–1131 (2009).
44. Manel, S., Poncet, B. N., Legendre, P., Gugerli, F. & Holderegger, R. Common factors drive adaptive genetic variation at different spatial scales in *Arabidopsis alpina*. *Mol. Ecol.* **19**, 3824–3835 (2010).
45. Zulliger, D., Schnyder, E. & Gugerli, F. Are adaptive loci transferable across genomes of related species? Outlier and environmental association analyses in Alpine Brassicaceae species. *Mol. Ecol.* **22**, 1626–1639 (2013).
46. Fang, J. Y. *et al.* Divergent selection and local adaptation in disjunct populations of an endangered conifer, *Keteleeria davidiana* var. *formosana* (Pinaceae). *PLoS One* **8**, e70162 (2013).
47. Holliday, J. A., Ritland, K. & Aitken, S. N. Widespread, ecologically relevant genetic markers developed from association mapping of climate-related traits in Sitka spruce (*Picea sitchensis*). *New Phytol.* **188**, 501–514 (2010).
48. Mosca, E. *et al.* The geographical and environmental determinants of genetic diversity for four alpine conifers of the European Alps. *Mol. Ecol.* **21**, 5530–5545 (2012).
49. Grivet, D., Sebastiani, F., Gonzalez-Martinez, S. C. & Vendramin, G. G. Patterns of polymorphism resulting from long-range colonization in the Mediterranean conifer Aleppo pine. *New Phytol.* **184**, 1016–1028 (2009).
50. Eckert, A. J. *et al.* Back to nature: ecological genomics of loblolly pine (*Pinus taeda*, Pinaceae). *Mol. Ecol.* **19**, 3789–3805 (2010).
51. Tsumura, Y., Uchiyama, K., Moriguchi, Y., Ueno, S. & Ihara-Ujino, T. Genome scanning for detecting adaptive genes along environmental gradients in the Japanese conifer. *Cryptomeria japonica*. *Heredity* **109**, 349–360 (2012).
52. Bigras, F. J. & Colombo, S. *Conifer cold hardiness*. (Springer Science & Business Media, 2001).
53. Blödner, C., Skroppa, T., Johnsen, O. & Polle, A. Freezing tolerance in two Norway spruce (*Picea abies* [L.] Karst.) progenies is physiologically correlated with drought tolerance. *J. Plant Physiol.* **162**, 549–558 (2005).
54. Bower, A. D. & Aitken, S. N. Ecological genetics and seed transfer guidelines for *Pinus albicaulis* (Pinaceae). *Am. J. Bot.* **95**, 66–76 (2008).
55. Chen, W. *et al.* The east-west zonal distribution of gymnosperm floras in China and the relationship with the main climatic factors. *Acta Sci. Natur. Univ. Sunyatseni* **52**, 130–139 (2013).
56. Sork, V. L. *et al.* Gene movement and genetic association with regional climate gradients in California valley oak (*Quercus lobata* Nee) in the face of climate change. *Mol. Ecol.* **19**, 3806–3823 (2010).
57. Li, C., Sun, Y., Huang, H. W. & Cannon, C. H. Footprints of divergent selection in natural populations of *Castanopsis fargesii* (Fagaceae). *Heredity* **113**, 533–541 (2014).
58. Cañas, R. A. *et al.* Understanding developmental and adaptive cues in pine through metabolite profiling and co-expression network analysis. *J. Exp. Bot.* **66**, 3113–3127 (2015).
59. Slatkin, M. *et al.* Linkage disequilibrium—understanding the evolutionary past and mapping the medical future. *Nat. Rev. Genet.* **9**, 477–485 (2008).
60. Neale, D. B. & Savolainen, O. Association genetics of complex traits in conifers. *Trends Plant Sci.* **9**, 325–330 (2004).
61. Dobzhansky, T. *Genetics of the evolutionary process*. (Columbia University Press, 1970).
62. Flint-Garcia, A. S., Thornsberry, M. J. & Buckler IV, S. E. Structure of linkage disequilibrium in plants. *Annu. Rev. Plant Biol.* **54**, 357–74 (2003).
63. Solomon, S. *et al.* IPCC fourth assessment report: the physical science basis. (2007) Available at: [http://www.ipcc.ch/publications\\_and\\_data/ar4/wg1/en/spmssp-projections-of.html](http://www.ipcc.ch/publications_and_data/ar4/wg1/en/spmssp-projections-of.html). (Accessed: 4th May 2015).
64. Davis, M. B. & Shaw, R. G. Range shifts and adaptive responses to Quaternary climate change. *Science* **292**, 673–679 (2001).
65. Hamann, A. & Wang, T. L. Potential effects of climate change on ecosystem and tree species distribution in British Columbia. *Ecology* **87**, 2773–2786 (2006).
66. Hamrick, J. L. *et al.* Response of forest trees to global environmental changes. *For. Ecol. Manage.* **197**, 323–335 (2004).
67. Burger, R. & Lynch, M. Evolution and extinction in a changing environment—a quantitative genetic analysis. *Evolution* **49**, 151–163 (1995).
68. Hijmans, R. J., Cameron, S. E., Parra, J. L., Jones, P. G. & Jarvis, A. Very high resolution interpolated climate surfaces for global land areas. *Int. J. Climatol.* **25**, 1965–1978 (2005).

69. Pan, H. W., Guo, Y. R., Su, Y. J. & Wang, T. Development of microsatellite loci for *Cephalotaxus Oliveri* (Cephalotaxaceae) and cross-amplification in *Cephalotaxus*. *Am. J. Bot.* **98**, e229–e232 (2011).
70. Yeh, F. C., Yang, R. & Boyle, T. POPGENE (version 1.31): Microsoft window-based freeware for population genetic analysis. Department of Renewable Resources, University of Alberta, Edmonton, Canada. URL [https://www.ualberta.ca/~fyeh/popgene\\_download.html](https://www.ualberta.ca/~fyeh/popgene_download.html) (1999).
71. Excoffier, L., Laval, G. & Schneider, S. Arlequin (version 3.0): An integrated software package for population genetics data analysis. *Evol. Bioinform.* **1**, 47–50 (2005).
72. Mantel, N. *et al.* The detection of disease clustering and a generalized regression approach. *Cancer Res.* **27**, 209–220 (1967).
73. Rousset, F. *et al.* Genetic differentiation and estimation of gene flow from F-statistics under isolation by distance. *Genetics* **145**, 1219–1228 (1997).
74. Nei, M. Estimation of average heterozygosity and genetic distance from a small number of individuals. *Genetics* **89**, 583–590 (1978).
75. Miller, M. P. Tools for Populations Genetic Analyses (TFPGA) (version 1.3): A windows program for the analysis of allozyme and molecular population genetic data. Department of Biological Sciences, Northern Arizona University, Flagstaff, United States of America. URL <http://www.marksgeneticsoftware.net/tfpga.htm/> (1997).
76. Pritchard, J. K., Stephens, M. & Donnelly, P. Inference of population structure using multilocus genotype data. *Genetics* **155**, 945–959 (2000).
77. Wang, R., Compton, S. G. & Chen, X. Y. Fragmentation can increase spatial genetic structure without decreasing pollen-mediated gene flow in a wind-pollinated tree. *Mol. Ecol.* **20**, 4421–4432 (2011).
78. Evanno, G., Regnaut, S. & Goudet, J. Detecting the number of clusters of individuals using the software STRUCTURE: a simulation study. *Mol. Ecol.* **14**, 2611–2620 (2005).
79. Bradbury, P. J. *et al.* TASSEL: software for association mapping of complex traits in diverse samples. *Bioinformatics* **23**, 2633–2635 (2007).
80. Buckler, E., Kroon, D., Casstevens, T., Bradbury, P. & Zhang, Z. W. *Trait analysis by association, evolution and linkage (TASSEL): user manual*. (USDA-ARS and the National Science Foundation, 2009).
81. Wang, Y. H. *et al.* Genetic structure and linkage disequilibrium in a diverse, representative collection of the C4 model plant, *Sorghum bicolor*. *G3-Genes Genom. Genet.* **3**, 783–793 (2013).
82. Phillips, S. J., Anderson, R. P. & Schapire, R. E. Maximum entropy modelling of species' geographic distributions. *Ecol. Model.* **190**, 231–259 (2006).
83. Ortega-Andrade, H. M., Prieto-Torres, D. A., Gomez-Lora, I. & Lizcano, D. J. Ecological and geographical analysis of the distribution of the mountain tapir (*Tapirus pinchaque*) in Ecuador: importance of protected areas in future scenarios of global warming. *PLoS One* **10**, e0121137 (2015).
84. Manel, S., Williams, H. C. & Ormerod, S. J. Evaluating presence-absence models in ecology: the need to account for prevalence. *J. Appl. Ecol.* **38**, 921–931 (2001).
85. Swets, J. A. *et al.* Measuring the accuracy of diagnostic systems. *Science* **240**, 1285–1293 (1988).

## Acknowledgements

We thank Huawei Pan and Jianjun Liu of School of Life Sciences, Sun Yat-sen University, for assistance with the collection of plant materials. This work was supported by the National Natural Science Foundation of China (31070594, 31370364, and 31570652), and Project of Department of Science and Technology of Zhuhai City, China (2012D0401990031).

## Author Contributions

T.W. designed and performed the experiments, and wrote the manuscript; Z.W. conducted data analysis and checked English grammar; F.X. performed the ISSR experiment; Y.S. contributed to the supervision of the work and wrote the manuscript. All authors read and approved the final version of the manuscript.

## Additional Information

**Supplementary information** accompanies this paper at <http://www.nature.com/srep>

**Competing financial interests:** The authors declare no competing financial interests.

**How to cite this article:** Wang, T. *et al.* Local adaptation to temperature and precipitation in naturally fragmented populations of *Cephalotaxus oliveri*, an endangered conifer endemic to China. *Sci. Rep.* **6**, 25031; doi: 10.1038/srep25031 (2016).



This work is licensed under a Creative Commons Attribution 4.0 International License. The images or other third party material in this article are included in the article's Creative Commons license, unless indicated otherwise in the credit line; if the material is not included under the Creative Commons license, users will need to obtain permission from the license holder to reproduce the material. To view a copy of this license, visit <http://creativecommons.org/licenses/by/4.0/>